Molecular Microbiology (2007) **65**(4), 1018–1033
doi:10.1111/j.1365-2958.2007.05844.x
First published online 21 July 2007

Cobalt chloride, a hypoxia-mimicking agent, targets sterol synthesis in the pathogenic fungus *Cryptococcus neoformans*

Hyeseung Lee,[1†] Clara M. Bien,[2†] Adam L. Hughes,[2] Peter J. Espenshade,[2] Kyung J. Kwon-Chung[1] and Yun C. Chang[1*]
[1]*Laboratory of Clinical Infectious Diseases, NIAID, NIH, Bethesda, MD 20892, USA.*
[2]*Department of Cell Biology, Johns Hopkins University School of Medicine, Baltimore, MD 21205, USA.*

Summary

We investigated the effects of the hypoxia-mimetic $CoCl_2$ in the pathogenic fungus *Cryptococcus neoformans* and demonstrated that $CoCl_2$ leads to defects in several enzymatic steps in ergosterol biosynthesis. Sterol defects were amplified in cells lacking components of the Sre1p-mediated oxygen-sensing pathway. Consequently, Sre1p and its binding partner Scp1p were essential for growth in the presence of $CoCl_2$. Interestingly, high copies of a single gene involved in ergosterol biosynthesis, *ERG25*, rescued this growth defect. We show that the inhibitory effect of $CoCl_2$ on *scp1*Δ and *sre1*Δ cells likely resulted from either an accumulation of non-viable methylated sterols or a decrease in the amount of ergosterol. Similar findings were also observed in the ascomycetous yeast, *Schizosaccharomyces pombe*, suggesting that the effects of $CoCl_2$ on the Sre1p-mediated response are conserved in fungi. In addition, gene expression analysis revealed limited overlap between Sre1p-dependant gene activation in the presence of $CoCl_2$ and low oxygen. The majority of genes similarly affected by both $CoCl_2$ and low oxygen were involved in ergosterol synthesis and in iron/copper transport. This article identifies the Sre1p pathway as a common mechanism by which yeast cells sense and adapt to changes in both $CoCl_2$ concentrations and oxygen levels.

Accepted 18 June, 2007. *For correspondence. E-mail ychang@niaid.nih.gov; Tel. (+1) 301 496 8839; Fax (+1) 301 480 3240. †These authors contributed equally to this work.

Introduction

Cryptococcus neoformans is a human fungal pathogen, which dwells in natural environments with ambient air such as soil surface, dehydrated pigeon droppings and decaying tree barks (Kwon-Chung and Bennett, 1992). *C. neoformans* is an obligatory aerobic fungus, which grows optimally at 21% oxygen (Odds *et al*., 1995). Despite this strong requirement for oxygen, *C. neoformans* can adapt to reduced oxygen levels in the human brain and can cause fatal infection in both immunocompromised and normal patients (Kwon-Chung and Bennett, 1992). Therefore, the mechanisms by which *C. neoformans* senses and adapts to low-oxygen conditions in order to establish infection is an important question towards understanding the pathobiology of this organism.

Mechanisms of sensing and adaptation to low oxygen have been extensively studied in the mammalian system. Not only does hypoxia represent a fundamental physiologic response, but it is also critical to the pathogenesis of the major causes of human mortality such as stroke and cancer. A great deal of progress has been made in the understanding of oxygen-regulated gene expression. The hypoxia-inducible transcription factor HIF-1 has been identified as a mediator of the cellular oxygen response that activates the expression of over 70 genes involved in adaptation to hypoxia (Goldberg *et al*., 1988; Wang and Semenza, 1993; Semenza, 2004). A HIF-1 homologue, however, has not been identified in fungi, suggesting that cellular oxygen-sensing pathways may vary greatly between mammals and fungi.

Recently, a novel oxygen-sensing pathway has been identified in the fission yeast *Schizosaccharomyces pombe. S. pombe* cells respond to environmental oxygen concentrations by sensing changes in sterol levels in cell membranes (Hughes *et al*., 2005). This response leads to changes in gene expression mediated by the homologues of mammalian SREBP (sterol regulatory element-binding protein) transcription factors and their binding partner SCAP (SREBP cleavage-activating protein), named Sre1 and Scp1 respectively (Hughes *et al*., 2005). Under low-sterol conditions, the mammalian SREBP–SCAP complex travels from the endoplasmic reticulum to the Golgi where

the N-terminal transcription factor domain of SREBP is proteolytically cleaved and released from the membrane. The activated form of SREBP then enters the nucleus and regulates the expression of more than 30 genes that participate in lipid homeostasis (Horton *et al*., 2003). In fission yeast, Sre1 is activated in response to low oxygen levels and Sre1 regulates genes involved in several oxygen-dependant biosynthetic pathways. Recent studies have identified homologues of SREBP and SCAP in *C. neoformans* where Sre1p also plays an important role in the regulation of sterol biosynthesis as well as adaptation to the host environment upon infection (Chang *et al*., 2007; Chun *et al*., 2007). Deletion of the *SRE1* in *C. neoformans* results in reduced growth under low-oxygen conditions *in vitro* and a significant reduction in virulence in the animal model (Chang *et al*., 2007). Thus, *C. neoformans* Sre1p is required for low oxygen adaptation and infection, revealing an important role for low oxygen sensing pathways in microbial pathogenesis.

Sterol biosynthetic pathways are conserved in eukaryotes, synthesizing cholesterol in mammals and ergosterol in fungi. As sterol biosynthesis is an essential process in many fungi, this pathway is the target of major classes of antifungal compounds currently employed to treat mycotic infections. Most of the basic research in defining the fungal ergosterol biosynthetic pathway and in determining the types of sterol molecules that support growth has been conducted in *Saccharomyces cerevisiae*, which lacks an apparent SREBP homologue (Lees *et al*., 1999). Sterol studies in *C. neoformans*, however, have focused primarily on the mechanisms of drug resistance while little is known about the molecular and genetic aspects of sterol synthesis in *Cryptococcus*. Furthermore, studies using clinical and environmental isolates have shown extensive diversity in sterol composition and synthesis among strains (Ghannoum *et al*., 1994; Currie *et al*., 1995). Thus, understanding the mechanisms involved in the *SRE1*-dependent low oxygen response and its regulation of ergosterol synthesis will further advance our understanding of the biology and pathogenicity of *C. neoformans.*

In mammalian systems, cobalt chloride ($CoCl_2$) has been used as a chemical agent that reportedly induces a biochemical and molecular response similar to that observed under low-oxygen conditions (Goldberg *et al*., 1987; Wang and Semenza, 1993; Wang *et al*., 2000; Huang *et al*., 2003; Grasselli *et al*., 2005). In this study, we investigate the effects of the hypoxia-mimetic $CoCl_2$ in *C. neoformans.* We demonstrate that $CoCl_2$ treatment leads to defects in several enzymatic steps in ergosterol biosynthesis. In comparison with previous experiments on gene expression under low-oxygen conditions (Chang *et al*., 2007), we found limited similarity in the transcriptional response to $CoCl_2$ and low oxygen, demonstrating that these treatments have distinct effects on cell physiology. We therefore propose that in *C. neoformans* the response to $CoCl_2$ mimics certain aspects of low oxygen by targeting enzymes in the sterol biosynthetic pathway. Due to this, $CoCl_2$ appears to be not an effective chemical to screen for all pathways involved in oxygen sensing, but may be useful in uncovering factors involved in the Sre1p-mediated response.

Results

SRE1 *is required for growth in the presence of $CoCl_2$*

Our recent study showed that deletion of *SRE1* and *SCP1* in *C. neoformans* resulted in reduced growth under low-oxygen conditions and that *SRE1* is required for virulence (Chang *et al*., 2007). To further investigate the role of the *SRE1* pathway in adaptation to low oxygen, we tested the use of $CoCl_2$ as a hypoxia mimetic in *C. neoformans.* Western blot analysis was performed to detect Sre1p cleavage activation in the presence of 100 μM $CoCl_2$ for increasing amounts of time. Figure 1A shows that antibody to the N-terminus of Sre1p specifically detected the ~110 kDa full-length Sre1p precursor under normal growth conditions. Upon addition of $CoCl_2$, wild-type cells rapidly accumulated the cleaved, N-terminal transcription factor domain of Sre1p. Therefore, similar to low oxygen, $CoCl_2$ induces the activation of the Sre1p pathway. In addition, expression of the *SRE1* transcript was induced upon $CoCl_2$ treatment in the wild-type strain and its induction was abolished when *SCP1* was deleted (Fig. 1B). These data suggest that Sre1p activates its own expression in the presence of $CoCl_2$. As $CoCl_2$ induces Sre1p activation, we next tested whether the Sre1p pathway is required for cell growth on $CoCl_2$. Wild-type, *sre1*Δ and *scp1*Δ cells were grown at 30°C on rich medium alone or rich medium containing 0.6 mM $CoCl_2$. While the *sre1*Δ and *scp1*Δ mutants grew similar to wild type on rich medium alone, they failed to grow in the presence of $CoCl_2$ (Fig. 1C). Together, these data indicate that the Sre1p pathway is essential in the presence of $CoCl_2$.

Transcriptional regulation by Sre1p upon $CoCl_2$ treatment

To identify potential Sre1p target genes involved in Sre1p-mediated adaptation to $CoCl_2$, we performed whole-genome microarray experiments comparing the transcriptional profile of the wild-type and *sre1*Δ cells in the presence of 0.6 mM $CoCl_2$. We chose to compare wild-type cells to *sre1*Δ cells instead of *scp1*Δ cells and to use the same method for data analysis as in the previous study (Chang *et al*., 2007) as it would allow a direct comparison with the low oxygen microarray data in

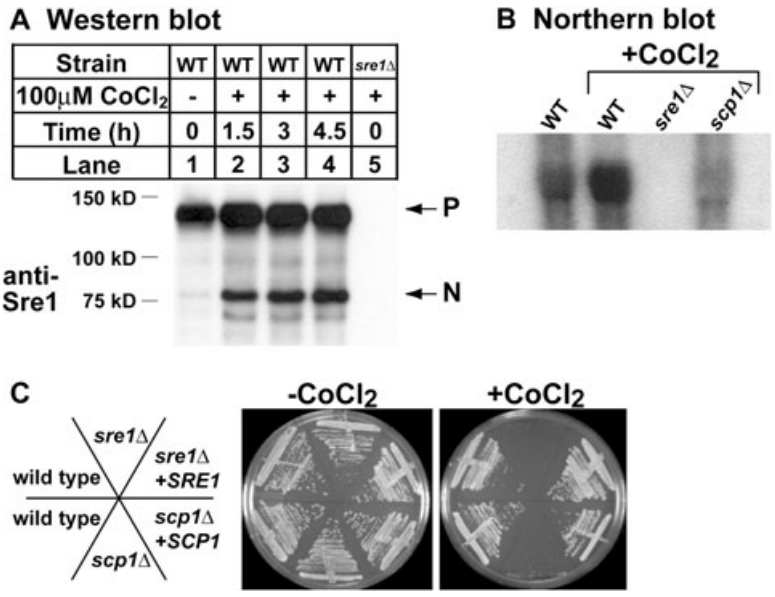

Fig. 1. *SRE1* expression is activated by $CoCl_2$ and *SRE1* is required for growth in the presence of $CoCl_2$.
A. Wild-type cells and the indicated mutant strains were cultured for the indicated time durations in YES medium containing 0.6 mM $CoCl_2$. Whole-cell extracts were prepared and subjected to immunoblot analysis using anti-Sre1p antiserum. P and N denote the precursor and cleaved nuclear forms of Sre1p respectively.
B. Total RNA was extracted from wild-type, *sre1*Δ and *scp1*Δ cultures grown in YES liquid medium without or with 0.6 mM $CoCl_2$ as indicated and hybridized with a *SRE1* probe.
C. Wild-type, mutant and complemented strains were streaked on YES or YES + 0.6 mM $CoCl_2$ as indicated. Plates were incubated at 30°C for 3 days.

C. neoformans. Cells were harvested after 2 h of $CoCl_2$ treatment to minimize complications due to indirect transcriptional effects caused by $CoCl_2$ treatment. All genes with statistically significant differences in expression between wild-type and *sre1*Δ cells were identified by significance analysis of microarray (SAM) using a mean false discovery rate (FDR) of less than 4% as described in *Experimental procedures* (Tusher *et al*., 2001).

Of the 6405 genes examined, 1111 genes (17%) showed a statistically significant difference between the wild-type and *sre1*Δ strains after $CoCl_2$ treatment. Of these 1111 genes, 366 genes were up- or downregulated by at least 1.8-fold. The majority (55%) of these genes were not annotated and do not have a significant homologue by BLAST search in any organism with an annotated genome. In Table 1, we classified the remaining 163 genes into different groups based on their annotated functions.

A total of 29 genes showed Sre1p dependence under low oxygen as well as $CoCl_2$ (Table 1, underlined genes). Interestingly, expression of many genes involved in the ergosterol synthesis and iron/copper transport was significantly higher in the wild-type strain compared with the *sre1*Δ strain in the presence of $CoCl_2$. This is consistent with previous data showing that *SRE1* is required for the upregulation of ergosterol biosynthetic genes and iron/copper transport genes under low oxygen (Chang *et al*., 2007). However, there was little overlap between the Sre1-dependant $CoCl_2$ data set and the low oxygen data set. For example, several different types of plasma membrane transporters, electron transport proteins, and proteins involved in fatty acid, carbohydrate and amino acid metabolism were more highly expressed in wild type versus *sre1*Δ under $CoCl_2$ treatment. These classes of genes did not appear to be differentially expressed between wild type and *sre1*Δ under low oxygen. It is possible that Sre1p controls a distinct set of target genes under $CoCl_2$ and low oxygen, or that many of these genes represent secondary effects of $CoCl_2$ on *sre1*Δ cells as compared with wild type. Collectively, these data reveal significant gene expression differences between wild-type and *sre1*Δ cells in the presence of $CoCl_2$.

ERG25 *suppresses* $CoCl_2$ *sensitivity in* scp1Δ *cells*

To test whether any single gene could bypass the requirement of the Sre1p pathway for growth on $CoCl_2$, we performed a multicopy suppressor screen. We generated a genomic library on a high-copy-number plasmid containing the *NAT* gene as a selectable marker. The multicopy genomic library was transformed into the *scp1*Δ strain by electroporation, and transformants were selected on medium containing 0.6 mM $CoCl_2$ and 100 μg ml^{-1} nourseothricin. In this initial screen, 23 clones were isolated from 1×10^6 transformants and confirmed to be $CoCl_2$ resistant. Eight of these suppressor plasmids coded for *SCP1* as determined by PCR using *SCP1*-specific primers. Episomal plasmids from each of the remaining clones were rescued in *Escherichia coli* and retransformed into the parent *scp1*Δ strain. Ten clones were successfully retested for $CoCl_2$ resistance and sequenced. Among these 10 clones, eight contained an overlapping sequence of *C. neoformans* genomic fragments ranging from 4.2 to 6.0 kb in size. This genomic DNA sequence was located on chromosome 3 and contained two putative genes: a hypothetical gene of unknown function (CNC02400) and a gene encoding C-4 methyl sterol oxidase, an *ERG25* homologue

Table 1. *SRE1*-dependent gene expression at 0.6 mM $CoCl_2$.

TIGR gene ID	Fold change[a] *sre1*Δ/WT	Description[b]
Ergosterol metabolism		
CNF04830	0.52	Hydroxymethylglutaryl-CoA reductase (*HMG1*)
CND01320	0.50	Electron transporter (*NCP1*)
CNA01070	0.46	C-14 sterol reductase (*ERG24*)
CND02520	0.43	Lanosterol synthase (*ERG7*)
CNG02670	0.37	Hydroxymethylglutaryl-CoA synthase (*ERG13*)
CNC04470	0.32	Delta2428 sterol reductase (*ERG4*)
CNF03720	0.30	C-22 sterol desaturase (*ERG5*)
CNB03100	0.30	Sterol 24-C-methyltransferase (*ERG6*)
CNC05280	0.30	Acetyl-CoA C-acetyltransferase (*ERG10*)
CNC05080	0.29	Hydroxymethylglutaryl-CoA synthase (*ERG13*)
CNA08290	0.28	C-8 sterol isomerase (*ERG2*)
CNA00300	0.28	Sterol 14-demethylase (*ERG11*)
CND06110	0.23	Squalene monooxygenase (*ERG1*)
CNA05010	0.17	C-5 sterol desaturase (*ERG3*)
CNC02410	0.17	C-4 methyl sterol oxidase (*ERG25*)
Sugar transport		
CNH02990	12.71	Sugar transporter
CNB02680	5.86	Glucose transporter
CNB03980	2.77	Hexose transport-related protein
CNJ03400	2.30	Hexose transport-related protein
CNH00540	2.30	Galactose transporter
CNC01940	1.84	Monosaccharide transporter
Other transporters		
CNE00260	2.89	Putative nicotinamide mononucleotide permease
CNK01330	2.81	Calcium ion transporter
CNE00390	2.40	Multidrug transporter
CNA07070	2.30	Dityrosine transporter
CNE00270	2.29	Amino acid transporter
CNI02800	2.20	Tartrate transporter
CNJ00070	1.91	Drug transporter
CNF04790	1.90	Transporter
CNM02030	0.48	Putative nicotinamide mononucleotide permease
CNM01030	0.40	Tricarboxylate carrier
CNF04560	0.39	Putative allantoate transporter
CNC03960	0.38	Phosphate transporter
CNC01330	0.35	Polyamine transport-related protein
CNL06680	0.34	Putative nicotinamide mononucleotide permease
CND02440	0.32	Peptide transporter
CNM02550	0.29	Putative uridine transporter
CND01860	0.28	Phospholipid transporter
CNE01880	0.15	transmembrane transporter Liz1p
CNM00800	0.04	Amino acid transporter
CND02430	0.03	Amino acid transporter
CNA02250	0.03	Ammonium transporter *MEP1*
CNI03510	0.01	Putative allantoate transporter
CND00530	0.01	Urea transporter
CNF01220	0.01	Putative allantoate transporter
Electron transport		
CNI02360	4.40	NADPH dehydrogenase 2
CNE03540	2.36	D-Lactaldehyde dehydrogenase
CND02380	2.29	Putative NADPH dehydrogenase
CNA01420	2.20	Oxidoreductase
CNB01620	0.49	L-Lactate dehydrogenase (cytochrome)
CNC05450	0.48	Oxidoreductase
CNF01310	0.44	Cytochrome P450
CND02060	0.22	Aldehyde dehydrogenase (ALDDH)
Fatty acid metabolism		
CNC05340	2.05	D-Arabinitol 2-dehydrogenase
CNB00370	0.55	Fatty acid beta-oxidation-related protein
CNE04360	0.54	Fatty acid synthase complex protein
Carbohydrate/amino acid metabolism		
CNA02580	3.53	Sorbitol dehydrogenase
CNJ00900	2.59	Enoyl reductase
CNB03180	2.56	Putative aromatic-amino-acid transaminase

Table 1. *cont.*

TIGR gene ID	Fold change[a] *sre1*Δ/WT	Description[b]
CNM00090	2.26	Glycoprotein
CNA07300	2.11	Enoyl reductase
CNN00460	0.49	Glycine dehydrogenase (decarboxylating)
CNC04350	0.48	Aminomethyltransferase, mitochondrial precursor
CNF01590	0.46	Aromatic-amino-acid transaminase
CNK00070	0.46	Phosphoketolase
CNE00820	0.45	Glycerol dehydrogenase
CNA03960	0.45	Glyoxal oxidase precursor
CNC01070	0.38	Glycine dehydrogenase mitochondrial precursor
CNI00870	0.37	Haloacid dehalogenase
CNA01850	0.34	Alcohol dehydrogenase
CNC06220	0.27	Glycerate- and formate-dehydrogenase
CNN01010	0.26	Malate dehydrogenase (oxaloacetate-decarboxylating)
CNN00990	0.26	Hydrolase
CNC02510	0.20	Beta-glucosidase
CNJ02910	0.16	Glutamate synthase (NADH)
CNE01840	0.15	General amidase
CNK00180	0.10	L-Serine ammonia-lyase
CNH02910	0.03	Malate synthase
CNC00920	0.02	Glutamate dehydrogenase ($NADP^+$)
Iron/copper transport		
CNI03410	3.29	Iron hydrogenase
CNG01900	2.21	Iron ion homeostasis-related protein
CNA02040	0.51	Ferric reductase transmembrane component
CND00150	0.32	Ferric-chelate reductase
CND01080	0.30	Copper uptake transporter
CNN00540	0.50	Solute carrier family 40; ferroportin 1
Other		
CNG01330	17.61	Pria protein precursor
CNB04110	10.64	CIP1 protein
CNC01660	6.95	Cytokine-inducing glycoprotein
CNG04630	5.21	Efflux protein EncT
CNM00910	4.24	Delayed-type hypersensitivity antigen-related
CNE00510	2.52	DNA repair protein rad16
CNC02920	2.51	Cytoplasm protein
CNJ00600	2.42	Response to drug-related protein
CND02630	2.39	Putative cytochrome *c* peroxidase
CNF02170	2.27	Endoplasmic reticulum protein
CNG03390	2.22	Yippe-like
CNK01600	2.11	RNA-binding protein
CNF02050	2.09	Sulphur metabolite repression control protein
CNB00160	2.08	Dehydrogenase
CNC02520	2.07	Chaperone, putative
CNM02290	2.04	Osmo-regulation-related protein
CND00480	2.01	Protein phosphatase inhibitor
CNL03990	2.00	Stomatin-like protein
CNE00890	1.99	Phosphoric monoester hydrolase
CNB00600	1.98	Cytoplasm protein
CNN01090	1.98	Cytoplasm protein
CNB03080	1.98	Nucleolus protein
CNL04270	1.97	DNA dependent ATPase
CND03510	1.92	Calcium-transporting ATPase
CNI04380	1.91	Glutathione S-transferase
CNA07780	1.91	Nicotinamidase
CNG03440	1.91	Yippe-like
CNA07860	1.89	ATP-dependent RNA helicase ded1
CNJ00220	1.89	RNA helicase
CNG01380	1.88	Hydrophilic protein
CNA07790	1.88	Calcineurin-binding protein-related
CNC03290	1.87	Tetracycline efflux protein
CND04160	1.87	RNA polymerase I transcription factor
CNB05450	1.85	rRNA processing-related protein
CNA03820	1.84	G1 phase of mitotic cell cycle-related protein
CNA01280	1.83	Monooxygenase
CNN02420	1.83	Receptor
CNC02490	1.82	Translational termination-related protein

Table 1. *cont.*

TIGR gene ID	Fold change[a] *sre1*Δ/WT	Description[b]
CNE04150	1.80	Mitochondrial protein
CNG00860	0.55	Mitochondial processing peptidase beta subunit
CNF03510	0.54	Mitochondrial protein
CNE02040	0.54	Uracil phosphoribosyltransferase
CNE05250	0.54	Enolase 1
CNG00600	0.54	Mannitol-1-phosphate dehydrogenase
CNA08130	0.53	2-Hydroxyacid dehydrogenase
CNH02350	0.53	Protein-histidine kinase
CNL05470	0.53	Alanine-glyoxylate transaminase
CNE03240	0.52	Chitin synthase
CNG00590	0.52	Folic acid and derivative metabolism-related protein
CNK02910	0.51	Aryl-alcohol dehydrogenase
CND02340	0.50	Allantoinase
CNI03480	0.50	Voltage-gated potassium channel beta-2 subunit
CNA07950	0.49	GTPase-activating protein
CNE00140	0.48	Transketolase
CNJ00800	0.48	Putative succinate-CoA ligase
CNL04840	0.48	Exo-beta-1,3-glucanase
CNK03000	0.46	Ubiquinone metabolism-related protein
CND03580	0.43	Chitin deacetylase
CNB03350	0.40	Multidrug resistance protein fnx1
CNG00350	0.40	Opsin 1
CNG04200	0.40	Alpha amylase
CNL05010	0.39	GabA permease
CNH01830	0.37	Arylformamidase
CNH02490	0.35	Cytoplasm protein
CNC06440	0.34	Inositol-3-phosphate synthase
CNA01820	0.33	Transcriptional activator
CNA02260	0.30	8-Amino-7-oxononanoatesynthase
CND02830	0.28	Nitrogen metabolism-related protein
CNH01900	0.26	Urease
CNA00680	0.26	Vacuole protein
CNI02420	0.24	Uricase (urate oxidase)
CNA05000	0.21	NADH dehydrogenase
CND00740	0.19	Allantoinase
CNJ01900	0.17	Cytoplasm protein
CNB04480	0.15	Carboxypeptidase s precursor
CNL05080	0.14	Putative transcription factor
CNF01380	0.10	Dihydropyrimidinase
CNL06330	0.02	Purine-cytosine permease

a. Data are presented as the average changes in expression of genes in *sre1*Δ treated with 0.6 mM $CoCl_2$ compared with their expression in wild type with 0.6 mM $CoCl_2$.
b. Descriptions were obtained from NCBI database (http://www.ncbi.nlm.nih.gov/) with additional hand editing.
List contains all functionally annotated, statistically significant genes identified by SAM that have average changes of greater than 1.8-fold in *sre1*Δ strain upon $CoCl_2$ treatment compared with wild type. Genes whose expression was shown to be at least 1.8-fold higher or lower in wild type versus *sre1*Δ at 1% O_2 treatment (Chang *et al*., 2007) are underlined.

(CNC02410). In addition to the *ERG25*-containing clones, one clone contained the N-terminal 625 amino acids of Sre1p, suggesting that this truncated *SRE1* gene may encode a Scp1p-independent, constitutively active form of Sre1p. The remaining one clone contained a gene encoding a putative 40S ribosomal protein. It is not clear how extra copies of this ribosomal protein gene can suppress the deficiency of Scp1p.

To define which gene from the rescued DNA fragments was responsible for suppression of the *scp1*Δ phenotype, an *ERG25*-containing DNA fragment was subcloned and retransformed into the *scp1*Δ strain. This fragment was sufficient to rescue the $CoCl_2$-sensitive phenotype of *scp1*Δ strain. Figure 2 shows that the *scp1*Δ strain transformed with a vector containing *ERG25* was resistant to $CoCl_2$ while the empty vector had no effect. Erg25p catalyses the removal of two C-4 methyl groups from intermediates in the ergosterol biosynthetic pathway and has been characterized in human, *S. cerevisiae*, *Candida albicans* and *S. pombe* (Bard *et al*., 1996; Li and Kaplan, 1996; Kennedy *et al*., 2000). Three distinct histidine-rich cluster motifs ($H^{170}X_3H$, $H^{183}X_2HH$, $H^{267}X_3H$) are conserved in all Erg25 proteins, and these motifs have been proposed to co-ordinate the iron atom(s) contained in these enzymes (Bard *et al*., 1996). According to the annotated sequence from the database (http://www.ncbi.nlm.nih.gov/entrez/), the 1.48 kb putative *CnERG25* ORF is comprised of five exons and four introns, and encodes a

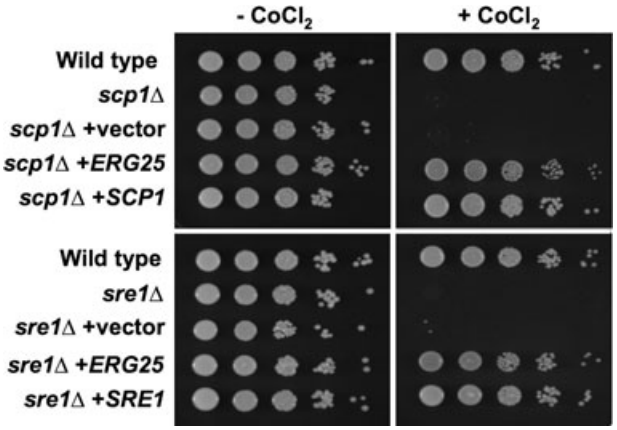

Fig. 2. Expression of *ERG25* rescues $CoCl_2$ sensitivity of *sre1*Δ and *scp1*Δ strains. Ten-fold serial dilutions of the indicated strains (30,000 to 3 cells) were spotted on YES and YES medium containing 0.6 mM $CoCl_2$ and incubated at 30°C for 3 days.

protein with a predicted molecular weight of 39.4 kDa. Sequence alignment of CnErg25p to other Erg25p homologues showed significant identity, particularly in the spacing and composition of the histidine-rich regions. The homology also extended outside the histidine regions (data not shown). These observations strongly suggest that CNC02410 is a homologue of *ERG25* in *C. neoformans*.

Scp1p and its orthologues have been shown to be required for proteolytic activation and processing of SREBPs in *C. neoformans*, fission yeast and mammalian cells (Rawson *et al*., 1999; Hughes *et al*., 2005; Chang *et al*., 2007). Due to this close association between Scp1p and Sre1p, we expect that overexpression of *ERG25* would also rescue the $CoCl_2$-sensitive phenotype of the *sre1*Δ strain. To test this possibility, we transformed *sre1*Δ cells with an *ERG25*-containing plasmid and tested for growth on 0.6 mM $CoCl_2$. Figure 2 shows that the *ERG25*-containing plasmid, but not the empty vector, rescued the $CoCl_2$ sensitivity of the *sre1*Δ strain. In addition, when the *ERG25* gene was transformed into either the *sre1*Δ strain or the *scp1*Δ strain as an integrated low-copy-number plasmid, as few as two additional copies of *ERG25* were sufficient for complementation of the $CoCl_2$ sensitivity of both *sre1*Δ and *scp1*Δ (data not shown). Thus, extra copies of *ERG25* rescued the growth defect of both *sre1*Δ and *scp1*Δ cells on $CoCl_2$ medium. Strains containing stably integrated *ERG25* were used for further study.

ERG25 *expression is upregulated upon* $CoCl_2$ *treatment via the Sre1p pathway*

Interestingly, our microarray experiments demonstrated that levels of *ERG25* transcript were 5.9-fold higher in wild-type cells than *sre1*Δ cells in the presence of $CoCl_2$ (Table 1). Thus, Sre1p may be required to increase levels of *ERG25* production to overcome the effects of $CoCl_2$. To test this, Northern blot experiments were performed to detect *ERG25* transcript levels in the absence and presence of $CoCl_2$. Figure 3A shows that $CoCl_2$ induces *ERG25* transcripts in wild-type cells. However, this induction is reduced in *sre1*Δ, *scp1*Δ and *sre1*Δ*scp1*Δ cells compared with that in wild type, confirming the microarray results. The low level of *ERG25* transcript detected in the deletion strains in the absence of $CoCl_2$ was increased by

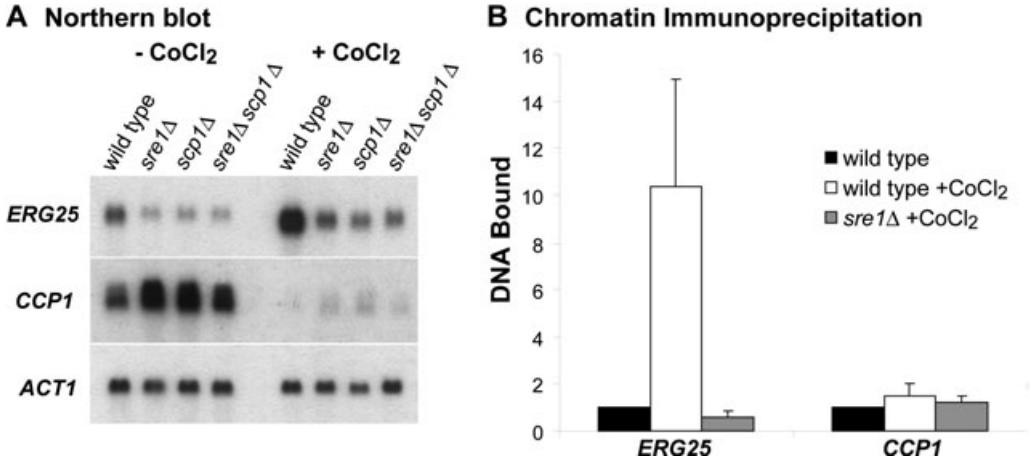

Fig. 3. Sre1p is recruited to the *ERG25* promoter in the presence of $CoCl_2$.
A. Total RNA was extracted from wild-type, *sre1*Δ, *scp1*Δ and *sre1*Δ*scp1*Δ cultures grown for 2 h in the absence or presence of 0.6 mM $CoCl_2$ and hybridized with *ERG25* and *CCP1*-specific probes. Actin (*ACT1*) served as a loading control.
B. Wild-type and *sre1*Δ cells were grown in the absence or presence of 0.6 mM $CoCl_2$ for 2 h. Chromatin immunoprecipitation was performed on formaldehyde-treated, sonicated cell extracts using anti-Sre1p polyclonal antibody. Fold change represents amount of immunoprecipitated DNA relative to the wild-type untreated sample. Error bars represent one standard deviation of fold changes in three biological replicate experiments.

addition of $CoCl_2$ although to a lesser extent than the wild-type strain. These data indicate that transcriptional regulator(s) in addition to Sre1p may control *ERG25* expression in response to $CoCl_2$. To address whether Sre1p is acting as a direct transcriptional regulator of *ERG25* under $CoCl_2$ treatment, we assayed Sre1p binding to the *ERG25* promoter using chromatin immunoprecipitation (Fig. 3B). Wild-type and *sre1*Δ strains were cultured in the absence and presence of 200 μM $CoCl_2$ for 2 h, and Sre1p-bound cross-linked DNA was isolated using polyclonal antibodies to Sre1p. Immunoprecipitated DNA was quantified using real-time PCR and primers directed to the promoter regions of *ERG25* and *CCP1*, which encodes a cytochrome *c* peroxidase. The amount of Sre1p bound to the *ERG25* promoter increased upon $CoCl_2$ treatment (10.3-fold). Expression of *CCP1* was upregulated in *sre1*Δ cells compared with wild type, suggesting that Sre1p may function to directly repress *CCP1* expression (Fig. 3A). However, Sre1p did not bind to the promoter region of *CCP1* (Fig. 3B) suggesting that the repression of *CCP1* expression was due to a secondary effect other than Sre1p binding to the promoter region of *CCP1*. Together, these data demonstrate that Sre1p activates the expression of *ERG25* by binding directly to its promoter in the presence of $CoCl_2$.

$CoCl_2$ targets sterol synthesis in C. neoformans

The fact that *ERG25* rescues the $CoCl_2$ sensitivity of the *scp1*Δ and *sre1*Δ strains and that Sre1p is activated by $CoCl_2$ suggests that $CoCl_2$ perturbs sterol biosynthesis. To investigate the impact of $CoCl_2$ on sterol synthesis, sterol compositions of wild-type and *scp1*Δ strains were determined by gas chromatography. First, we analysed the sterol profiles of wild-type cells grown in the absence or presence of 100 μM $CoCl_2$ for 6 h (Fig. 4A and B). Cells treated with $CoCl_2$ showed a dramatic accumulation of the Erg25p substrates, 4,4-dimethylfecosterol and 4-methylfecosterol. In addition, $CoCl_2$-treated cells also displayed increased amounts of the Erg3p and Erg4p substrates, episterol and tetraenol, and decreased amounts of Erg5p substrate, trienol. It is difficult to determine the extent of inhibition at these later steps in the pathway, as the amount of available substrates for Erg3p, Erg4p and Erg5p may be affected due to inhibition of the earlier step catalysed by Erg25p (Fig. 4A). Overall, these changes are consistent with blocks at several enzymatic steps in the sterol synthesis pathway, including Erg25p. As a consequence, wild-type cells treated with $CoCl_2$ contained less ergosterol than untreated cells (Fig. 4B). Second, we compared the sterol profiles of wild-type and *scp1*Δ cells without $CoCl_2$ treatment (Fig. 4C). Similar to our previous findings in the *sre1*Δ strain (Chang *et al*., 2007), *scp1*Δ cells contained slightly elevated levels of Erg25p substrates. Third, we compared sterol profiles of $CoCl_2$-treated wild-type and *scp1*Δ cells (Fig. 4D). $CoCl_2$-treated *scp1*Δ cells contained significantly lower levels of ergosterol and accumulated even higher levels of 4,4-dimethylfecosterol and 4-methylfecosterol than $CoCl_2$-treated wild-type cells. The *scp1*Δ cells also contained higher levels of other intermediates, such as lanosterol, 24-methylene lanosterol and episterol. In *S. cerevisiae*, deletion of *ERG2*, *ERG3*, *ERG4* or *ERG5* is not lethal while *ERG25* is essential (Lees *et al*., 1995). This suggests that the 4-methyl sterols, substrates for Erg25p, are either toxic or unable to support cell growth. In *C. neoformans*, *scp1*Δ cells accumulate higher levels of these 4-methyl intermediates than wild-type cells, possibly explaining the inability of this strain to grow in the presence of $CoCl_2$. These data indicate that *SCP1* is required to maintain sterol homeostasis under the influence of $CoCl_2$.

To test whether *ERG25* rescues growth of *scp1*Δ cells on $CoCl_2$ by lowering 4-methyl sterol levels, we carried out time-course experiments to test the effects of $CoCl_2$ on sterol synthesis of wild-type, *scp1*Δ, *SCP1*-complemented *scp1*Δ and *scp1*Δ+*ERG25* strains (Fig. 5). The *scp1*Δ strain accumulated significantly higher amounts of 4,4-dimethylfecosterol and 4-methylfecosterol upon $CoCl_2$ treatment over time compared with the wild-type strain and the *SCP1*-complemented *scp1*Δ strain (Fig. 5A and B). Interestingly, 4,4-dimethylfecosterol and 4-methylfecosterol did not accumulate in the *ERG25*-transformed *scp1*Δ strain compared with either the wild-type strain or *SCP1*-complemented *scp1*Δ strain. However, two intermediates downstream of Erg25p substrates, episterol and tetraenol, did accumulate to high levels over time in the *ERG25*-transformed *scp1*Δ strain, suggesting that $CoCl_2$ leads to an inhibition of Erg3p and Erg4p (Fig. 5C and D). One reason these defects were not seen in the other strains may be due to an upstream block at Erg25p in the presence of $CoCl_2$. We did not observe a significant increase in the level of trienol in the *ERG25*-transformed *scp1*Δ strain, which suggests that Erg5p is unlikely to be affected by $CoCl_2$ (data not shown). We also analysed sterols of the *sre1*Δ strain set (wild type, *sre1*Δ, *ERG25*- and *SRE1*-transformed *sre1*Δ strain) and observed similar results (data not shown). Taken together, these data suggest that the failure of *scp1*Δ and *sre1*Δ cells to grow on $CoCl_2$ may be due to either an accumulation of non-viable methylated sterols or a decrease in the amount of ergosterol.

ERG25 *rescues $CoCl_2$ sensitivity of* S. pombe sre1Δ *strain*

To determine whether $CoCl_2$ inhibits sterol synthesis in other fungi, we examined the effects of $CoCl_2$ in the fission yeast *S. pombe*. Western blot analysis showed that

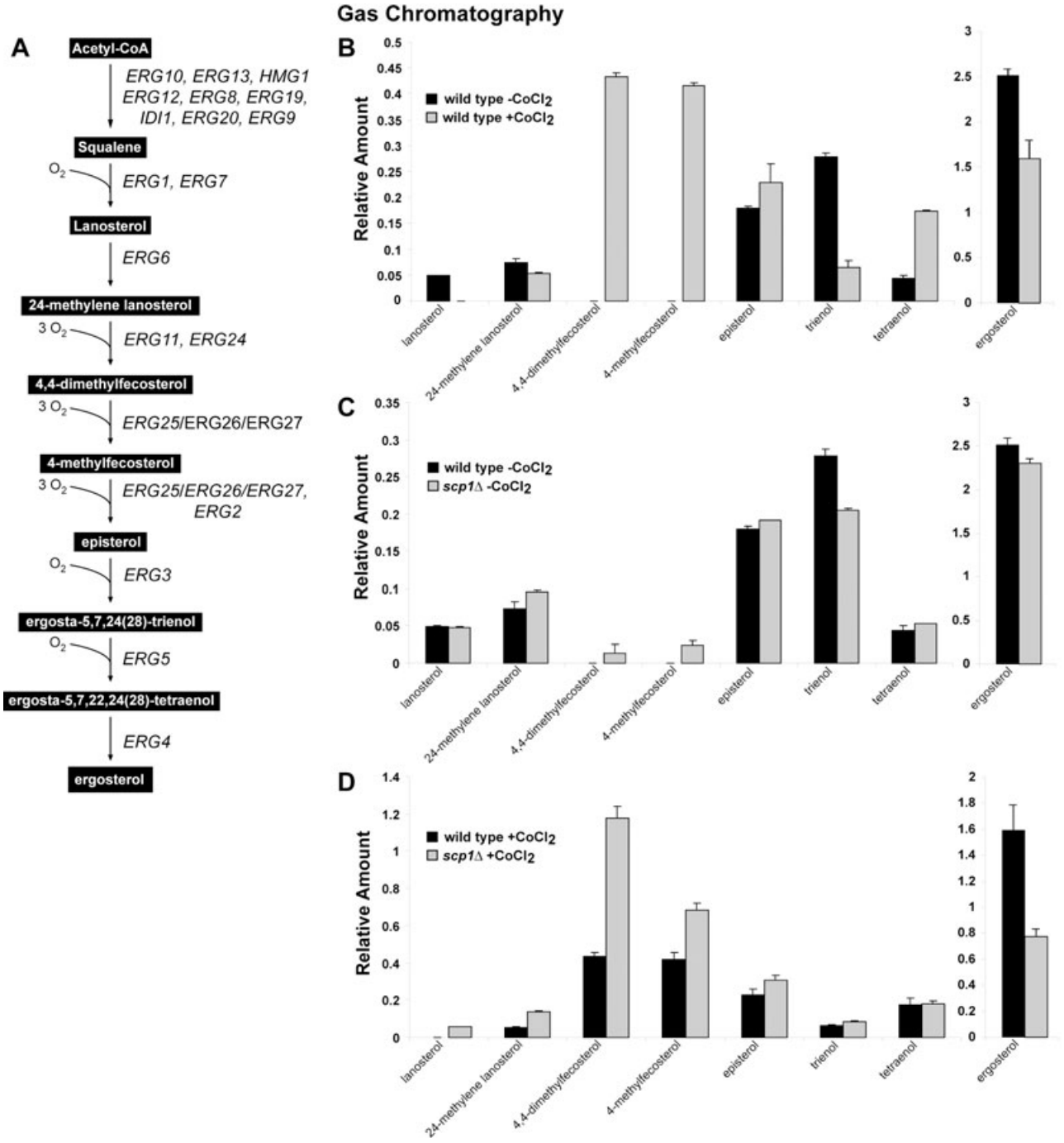

Fig. 4. $CoCl_2$ inhibits ergosterol synthesis. The indicated strains were grown in the absence or presence of 100 μM $CoCl_2$ for 2 h. Sterols were extracted and subjected to gas chromatography analysis. Relative amounts of each intermediate were determined by normalizing to an internal cholesterol standard.

A. Putative ergosterol biosynthetic pathway in *C. neoformans*.

B. Comparison of wild-type cells in the absence and presence of $CoCl_2$.

C. Comparison of untreated wild-type and *scp1*Δ strains.

D. Comparison of $CoCl_2$-treated wild-type and *scp1*Δ strains.

In all graphs, trienol and tetraenol are used as an abbreviation for ergosta-5,7,24(28)-trienol and ergosta-5,7,22,24(28)-tetraenol respectively.

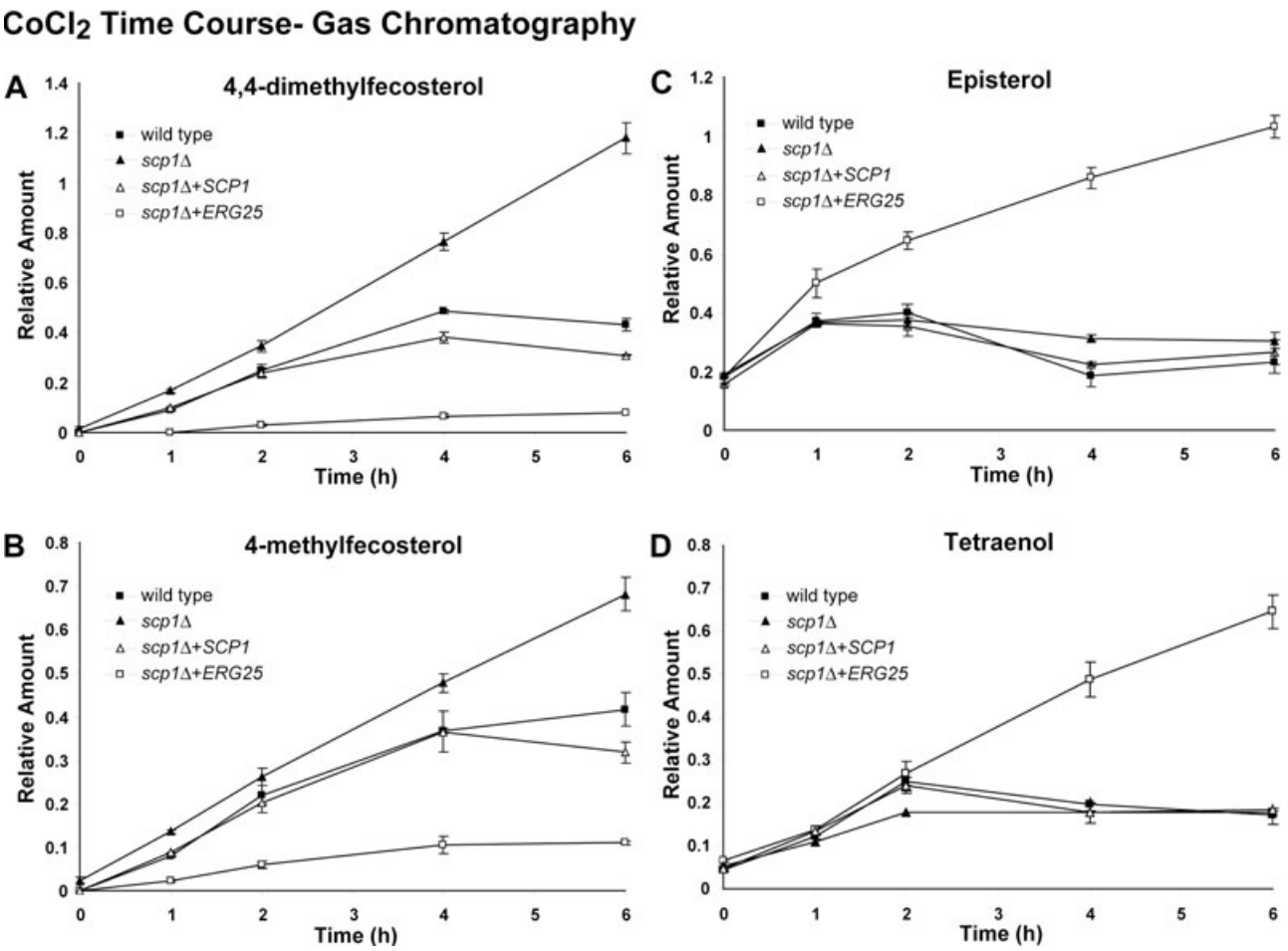

Fig. 5. Extra copies of *ERG25* block the accumulation of methylated sterol intermediates in $CoCl_2$ treatment. Cells from the four different strains were grown for 0, 1, 2, 4 and 6 h in the presence of 100 μM $CoCl_2$. Sterols were extracted and subjected to gas chromatography analysis. Relative amounts of each intermediate were determined by normalizing to an internal cholesterol standard. Changes in the relative amount of (A) 4,4-dimethylfecosterol, (B) 4-methylfecosterol, (C) episterol and (D) ergosta-5,7,22,24(28)-tetraenol were plotted over the time of $CoCl_2$ treatment.

treatment of wild-type *S. pombe* cells with 200 μM $CoCl_2$ activated SpSre1 cleavage and resulted in the accumulation of the N-terminal nuclear form of SpSre1 as observed in *C. neoformans* (Figs. 6A and 1A). In addition, a *S. pombe sre1*Δ strain grew poorly on 1.6 mM $CoCl_2$ compared with the wild-type strain and this sensitivity was rescued by overexpression of *erg25*$^+$ (Fig. 6B). Wild-type cells treated with 200 μM $CoCl_2$ also contained decreased amount of ergosterol and elevated amounts of several sterol pathway intermediates including the Erg25 substrates, 4,4-dimethylfecosterol and 4-methylfecosterol (Fig. 6C). These data suggest that $CoCl_2$-mediated inhibition of ergosterol production and $CoCl_2$-induced activation of SREBP is conserved across phyla in the fungal kingdom.

Discussion

This study investigated the role of $CoCl_2$ as a hypoxia-mimicking agent in the pathogenic fungus *C. neoformans*. Here, we report important differences and similarities between cellular responses to low oxygen and $CoCl_2$. Collectively, our data show that the Sre1p-mediated response is induced by $CoCl_2$, suggesting a role for Sre1p in the adaptation to high levels of $CoCl_2$.

Although cobalt has been widely used as a hypoxia-mimicking agent in mammalian systems, the mechanism by which it induces hypoxia-mimicking responses is not fully understood. In this article, we demonstrate that $CoCl_2$ leads to defects in several enzymatic steps in ergosterol biosynthesis in *C. neoformans*. Interestingly, two of the inhibited steps are catalysed by iron (II)-dependant, oxygen-requiring enzymes Erg25p and Erg3p. It is known that cobalt (II) and nickel (II) can be incorporated into haemoproteins, which normally contain iron (II) to co-ordinate oxygen molecules, including cytochrome P450 enzymes (Sinclair *et al.*, 1979; 1982). In addition, cobalt (II) has also been shown to inhibit oxygen-requiring enzymes containing non-haem-iron molecules, such as

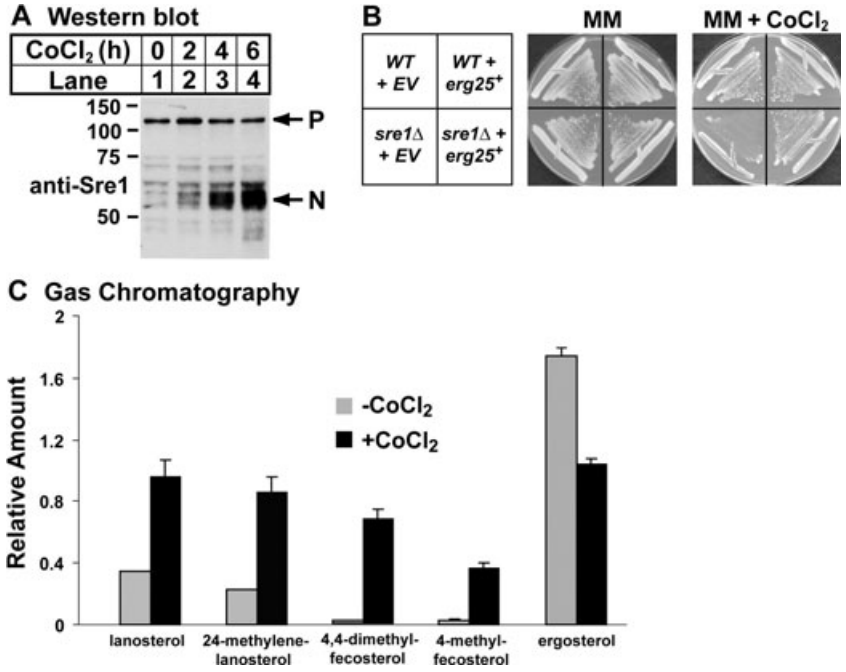

Fig. 6. Sre1-dependant adaptation to $CoCl_2$ is conserved in the fission yeast, *S. pombe*.
A. Wild-type *S. pombe* cells were grown in the presence of 200 μM $CoCl_2$ for increasing amounts of time. Cells extracts were subjected to immunoblot analysis using anti-Sre1 polyclonal antibody.
B. The indicated strains were grown on solid minimal medium (MM) alone or in the presence of 1.6 mM $CoCl_2$ at 30°C.
C. Wild-type cells were grown for 6 h in the absence or presence of 200 μM $CoCl_2$ and subjected to sterol analysis by gas chromatography.

asparaginyl and prolyl hydroxylases (Epstein *et al*., 2001; Hewitson *et al*., 2002). Unlike iron, cobalt (II) and nickel (II) have a lower affinity for oxygen than iron (II) (Shibayama *et al*., 1986). Therefore, cobalt and nickel may simulate hypoxia by directly inhibiting oxygen-requiring enzymes. For instance, $CoCl_2$ stabilizes HIF-1α subunits by preventing the binding of oxygen molecules to the HIF prolyl hydroxylases, and subsequent HIF-1α hydroxylation and degradation by the proteosome (Bruick and McKnight, 2001; Jaakkola *et al*., 2001; Semenza, 2004).

In yeast, ergosterol biosynthesis requires two cytochrome P450 enzymes, Erg11p and Erg5p. Interestingly, these enzymes do not appear to be inhibited by $CoCl_2$ in *C. neoformans*. Instead, two oxygen-dependant di-iron-containing enzymes, Erg25p and Erg3p, displayed greater inhibition by $CoCl_2$. This suggests that di-iron-containing non-haem proteins may be more vulnerable to metal substitution than haem-containing enzymes in *C. neoformans*. Thus, our studies on the hypoxia-mimicking effects of $CoCl_2$ in *C. neoformans* provide an interesting parallel to mammalian systems.

Our previous work identified an oxygen-sensing mechanism in *C. neoformans*, in which the transcription factor Sre1p is required for normal growth under low oxygen (Chang *et al*., 2007). Here, we show that $CoCl_2$ activates Sre1p, and that components of the Sre1p pathway, Sre1p and Scp1p, are required for growth in the presence of $CoCl_2$. However, the similarities between Sre1p-dependant transcriptional responses to low oxygen and $CoCl_2$ are limited. Previous studies on low-oxygen gene expression identified 41 genes whose expression was greater than 1.8-fold higher in wild-type cells than *sre1*Δ cells at 1% oxygen, including 19 genes involved in ergosterol biosynthesis and iron/copper homeostasis (Chang *et al*., 2007). In contrast, microarray experiments comparing wild-type and *sre1*Δ cells in the presence of $CoCl_2$ revealed many more Sre1p-dependant genes than under low oxygen, including 98 genes at least 1.8-fold more highly expressed in wild-type cells and 65 genes at least 1.8-fold more highly expressed in *sre1*Δ cells. Among the 163 $CoCl_2$-affected genes listed in Table 1, only 29 genes were also affected in the low oxygen-treated cells (18%; Table 1 underlined genes). Overall, the total number of Sre1p-dependant genes in the presence of $CoCl_2$ was greater than under low oxygen (1111 versus ~500). This may be due to a greater requirement for the Sre1p pathway in the presence of $CoCl_2$. This idea is supported by the fact that *sre1*Δ and *scp1*Δ cells show a more dramatic growth defect on $CoCl_2$ than under low oxygen compared with wild-type cells. On plates containing 0.6 mM $CoCl_2$, the *sre1*Δ and *scp1*Δ strains showed complete growth inhibition, while residual growth of the *sre1*Δ and *scp1*Δ strains was detectable in hypoxic conditions (1% O_2) (Chang *et al*., 2007). Thus, the cellular response to low oxygen and $CoCl_2$ appear to be different in *C. neoformans* and $CoCl_2$ may provide a more restrictive condition for identification of novel Sre1p pathway components. Consistent with our data, recent analysis of gene expression in mammalian fibroblast showed only 19% overlap between $CoCl_2$- and hypoxically induced genes (Vengellur *et al*., 2003). This indicates that although $CoCl_2$ has been widely used as a hypoxia-

mimicking agent, similarity between the transcriptional responses to low oxygen and $CoCl_2$ is limited.

It is noted that, in addition to ergosterol biosynthetic and iron/copper metabolic genes, the genes involved in fatty acid catabolism were also reproducibly affected, although changes in their expression were not as dramatic as those of the ergosterol biosynthetic genes (Table 1 and Table S1). Interestingly, SREBP orthologues are known to regulate genes involved in fatty acid metabolism, suggesting that the co-regulation of sterols and fatty acids may be conserved in *C. neoformans* (Bennett *et al*., 1995). In addition, numerous plasma membrane transporter genes involved nicotinamide, allantoate, phospholipid, amino acid and ammonium transport were upregulated in a *SRE1*-dependant manner in the presence of $CoCl_2$. These genes have not previously been shown to be targets of SREBP in other systems.

Differences in gene expression between *sre1*Δ and wild-type cells in the presence of $CoCl_2$ may represent secondary responses to $CoCl_2$ due to changes in membrane sterol composition. Ergosterol is responsible for maintaining the shape and rigidity of cell membranes, and it has been postulated that defects in ergosterol biosynthesis may lead to changes in membrane stiffness (Theis and Stahl, 2004). Therefore, by disrupting sterol synthesis, $CoCl_2$ may affect membrane properties including fluidity, transport functions and membrane enzyme activities (Burger *et al*., 2000). Defects in these properties may then signal transcriptional changes of membrane-associated genes. Lastly, several electron transporters were differentially regulated in *sre1*Δ cells in the presence of $CoCl_2$. Besides activation of a hypoxic response, $CoCl_2$ has been proposed to generate reactive oxygen species and deplete ascorbate in mammalian cells (Salnikow *et al*., 2004; Grasselli *et al*., 2005; Triantafyllou *et al*., 2006). It is possible that Sre1p may be required for cells to adapt to redox perturbations in response to $CoCl_2$ treatment.

Despite the fact that $CoCl_2$ inhibits several steps in ergosterol biosynthesis, we found that additional copies of a single gene, *ERG25*, were sufficient to rescue growth of *sre1*Δ and *scp1*Δ cells on $CoCl_2$. In contrast, extra copies of *ERG25* were unable to rescue growth of the mutants under low oxygen (data not shown), further reinforcing the difference between the effects of low oxygen and $CoCl_2$. *ERG25* expression is upregulated by $CoCl_2$ in a Sre1p-dependant manner, and chromatin immunoprecipitation experiments demonstrated that *ERG25* is a direct target of Sre1p. The fact that *ERG25* rescues growth of *sre1*Δ and *scp1*Δ cells on $CoCl_2$ suggests that, in contrast to low oxygen, Erg25p is the major Sre1p-dependant factor that is limiting for growth on $CoCl_2$.

Sterol analysis revealed that $CoCl_2$ treatment leads to increased levels of several sterol intermediates, including the substrates of Erg25p, 4,4-dimethylfecosterol and 4-methylfecosterol, demonstrating that Sre1p regulates sterol homeostasis in response to $CoCl_2$. The accumulation of 4-methyl sterols was abolished in *sre1*Δ and *scp1*Δ cells expressing extra copies of *ERG25*. As Erg25p was sufficient to rescue growth of the *scp1*Δ strain on $CoCl_2$, it is likely that Erg25p substrates are functionally different from other sterol pathway intermediates. Consistent with this finding, it has previously been shown in *S. cerevisiae* that deletion of *ERG2*, *ERG3*, *ERG5* and *ERG4* in the sterol synthesis pathway does not cause lethality. However, Erg25p and all other upstream enzymes are essential for growth in the absence of ergosterol supplement (Lees *et al*., 1995; Gachotte *et al*., 1998; 1999). Thus, it is possible that sterol intermediates containing C-4 methyl groups cannot support growth, and that cells are only able to survive on sterols that have undergone the C-4 demethylation steps catalysed by Erg25p.

In this study, we have demonstrated that the oxygen-sensing transcription factor Sre1p is required for adaptation to $CoCl_2$. Upon $CoCl_2$ treatment, Sre1p is likely activated in response to sterol defects caused by the inhibition of several enzymatic steps in the ergosterol biosynthetic pathway. $CoCl_2$-induced sterol synthesis inhibition and Sre1p activation was also observed in *S. pombe*, suggesting a conserved role for Sre1p in the adaptation to elevated levels of transition metals. Due to high conservation of many sterol biosynthetic enzymes, $CoCl_2$ may also have similar effects on sterol synthesis in mammalian systems.

Experimental procedures

Strains, media and growth conditions

All *C. neoformans* strains used in this study were of serotype D and are listed in Table 2. Strains used were all derived from B-3501A, one of the *C. neoformans* serotype D genomic sequencing strains (http://www-sequence.stanford.edu/group/C.neoformans/index.html). The strains were maintained on YES medium. YES medium contains 0.5% (w/v) yeast extract plus 3% glucose and supplements consisted of 225 μg ml^{-1} each of uracil, adenine, leucine, histidine and lysine (Moreno *et al*., 1991). *S. pombe* strains were derived from KGY425 wild-type strain. Culture conditions and methods for cell extract preparation, Sre1p cleavage assays, sterol analysis and yeast transformation were previously described (Hughes *et al*., 2005).

Multicopy suppressor library construction

The multicopy suppressor library was constructed as follows. Genomic DNA from the serotype D *MAT*a strain LP2 (Lee *et al*., 2005) was partially digested with Sau3A and the cohesive ends were half-filled in with dATP and dGTP using Klenow DNA polymerase. Genomic DNA fragments ranging from 5 to 12 kb were ligated into XhoI-digested vector,

Table 2. List of strains relevant to this study.

Strains	Genotype	Reference
B-3501A	*MAT*α, parent of B-4478 and B-4476	Kwon-chung *et al.* (1992)
C814	*MAT*α, *scp1*Δ*::NEO*	Chang *et al.* (2007)
C1037	*MAT*α, *sre1*Δ*::NAT*	Chang *et al.* (2007)
HL133	*MAT*α, *sre1*Δ*::NAT* + *ERG25::NEO*	This study
HL134	*MAT*α, *sre1*Δ*::NAT* + pYCC726 (*NEO*)	This study
HL135	*MAT*α, *scp1*Δ*::NEO* + *ERG25::NAT*	This study
HL136	*MAT*α, *scp1*Δ*::NEO* + pYCC725 (*NAT*)	This study
C1051	*MAT*α, *sre1*Δ*::NAT* + *SRE1::NEO*	Chang *et al.* (2007)
C1046	*MAT*α, *scp1*Δ*::NEO* + *SCP1::NAT*	Chang *et al.* (2007)
C826	*MAT*α, *scp1*Δ*::NEO*, *sre1*Δ*::NAT*	This study
S. pombe KGY425	*h-, his3-D1, leu1-32, ura4-D18, ade6-M210*	Burke and Gould (1994)
S. pombe PEY522	*h-, sre1*Δ*::NEO, his3-D1, leu1-32, ura4-D18, ade6-M210*	Hughes *et al.* (2005)

pYCC725. The XhoI site of pYCC725 was half-filled in with dCTP and dTTP before ligation. pYCC725 is similar to a telomere-containing plasmid that is episomally maintained in multiple copies in *C. neoformans* (Mondon *et al.* 2000) and provides functional overexpression of cloned genes using nourseothricin resistance as a selection. The genomic library was linearized with I-SceI and transformed into the *scp1*Δ strain, C814, by electroporation as described previously (Edman and Kwon-Chung, 1990). As the original *sre1*Δ strain was generated using a *NAT* marker and the *scp1*Δ strain was generated with a *NEO* marker, we chose the *scp1*Δ strain for suppressor screening. Transformants were grown on medium containing 100 μg ml^{-1} nourseothricin and 0.6 mM $CoCl_2$. Total DNA was extracted from transformants that were able to grow on plates containing 0.6 mM $CoCl_2$. The inserts in the episomes were PCR-amplified using primers OYC725B and OYC725C that recognized pYCC725 vector sequences flanking the XhoI restriction site.

Expression of ERG25

In order to test the ability of *ERG25* to rescue growth of *scp1*Δ cells on $CoCl_2$, the 3.5 kb ApaI and NcoI fragment containing the *ERG25* gene in the original clone (pHL97) was subcloned into pYCC725 to yield pHL98. To obtain stable transformants, pHL98 was linearized with NotI to remove telomeres and retransformed into the *scp1*Δ or *sre1*Δ strain by biolistic transformation. Integration events and copy number were confirmed by Southern blot analysis. Vector control strains were similarly obtained by transforming the NotI digested pYCC725. *S. pombe* strain containing nmt*-3xHA-erg25, encoding *erg25*$^+$ preceded by three copies of the HA tag under control of the nmt* promoter, was generated by insertion of 3xHA into Rep41X followed by insertion of *erg25*$^+$ open reading frame amplified from *S. pombe* genomic DNA with Pfu Ultra polymerase (Forsburg, 1993).

Preparation and analysis of nucleic acid

Isolation and analysis of genomic DNA was carried out as described previously (Chang and Kwon-Chung, 1994). For RNA extraction, cells grown under the indicated conditions were harvested and cell pellets were frozen on dry ice/ethanol, lyophilized for 15 h and then lysed by glass bead beating. RNA was extracted from yeast cells using Trizol (Invitrogen, Carlsbad, CA), and purified with RNeasy MinElute cleanup kit (Qiagen, Valencia, CA). PCR fragments (1–1.4 kb) used for Northern probes were generated using gene-specific primers. The 3.5 kb NcoI and ApaI fragment from pHL97 was used as the *ERG25* probe. Radioactive probes were prepared using StripEZ kit (Ambion, Austin, TX) according to manufacturer's manual. Northern blot analysis was performed as described previously (Chang *et al.*, 1995).

Antibody preparation

A plasmid expressing *C. neoformans* Sre1p amino acids 1–320 and a 6x Histidine epitope tag was transformed into *E. coli*. Antigen was purified from *E. coli* using Ni-NTA Agarose beads (Qiagen, Valencia, CA). Rabbits were immunized with antigen and serum was extracted using a standard protocol (Covance, Princeton, NJ).

Cell extract preparation

Cryptococcus neoformans cells were grown in YES medium under the indicated conditions. A total of 4×10^7 cells were washed in sterile H_2O and lysed by glass bead beating (425–600 mm, Sigma, St Louis, MO) in 25 mM NaOH and 128 mM 2-mercaptoethanol. Proteins were precipitated with 6.4% (w/v) trichloroacetic acid followed by two acetone washes. Proteins were re-suspended in SDS lysis buffer [1% (w/v) SDS, 10 mM Tris-HCl (pH 6.8), 1 mM EDTA, 1 mM EGTA] plus protease inhibitors (25 μg ml^{-1} ALLN, 10 μg ml^{-1} leupeptin, 2 μg ml^{-1} aprotinin, 5 μg ml^{-1} pepstatin A, 0.5 μg ml^{-1} PMSF and 1 mM DTT).

Immunoblot analysis

Immunoblot experiments using *C. neoformans* and *S. pombe* cell extracts were performed as described previously (Hughes *et al.*, 2005; Chang *et al.*, 2007).

Sterol analysis

Sterols were extracted from 1×10^8 log-phase cells grown under the indicated conditions. Cells were washed with

sterile H_2O and collected by centrifugation. Pellets were re-suspended in 9 ml of methanol, 4.5 ml of 60% (w/v) KOH and 5 μg of cholesterol (used as an internal recovery standard). Cells were then saponified for 2 h at 75°C with agitation. Samples were cooled to room temperature and extracted with 4 ml of petroleum ether. Solid sterols were recovered by evaporation of the petroleum ether under a stream of nitrogen gas. Sterols were re-suspended in 200 μl of heptane and 2 μl were injected into an Agilent 6850 gas chromatograph with an HP-1 column and FID. Retention times for sterol intermediates were determined using standards.

Plate assays

Exponentially growing cultures (OD_{600} = 0.5–1.0) were washed, re-suspended in 0.9% NaCl and adjusted to OD_{600} = 0.5. Adjusted cell suspensions were serially diluted and spotted onto YES agar medium supplemented with $CoCl_2$ at the indicated concentrations. Incubation was at 30°C for 3–4 days.

Microarray experiments

Microarray slides were purchased from the Genome Sequencing Center at Washington University. Overnight cultures of wild-type (B-3501A) and *sre1*Δ strains were refreshed and grown in YES for 5 h and incubated for an additional 2 h in the presence or absence of 0.6 mM $CoCl_2$. RNA was extracted from yeast cells using Trizol (Invitrogen, Carlsbad, CA), treated with RNAse-free Dnase (Ambion, Austin, TX) for the removal of genomic DNA, and purified with RNeasy MinElute cleanup kit (Qiagen, Valencia, CA). cDNA labelled with Cyanine 3 (Cy3) or Cyanine 5 (Cy5) (Amersham, Piscataway, NJ) was synthesized with FairplayII Microarray Labelling Kit (Stratagene, La Jolla, CA) according to manufacturer's manual and subjected to competitive hybridization on the microarray. cDNAs from wild-type and *sre1*Δ strains were labelled with Cy3 and Cy5, respectively, and the dyes were reversed for the reverse fluor control. Cy3-cDNA and Cy5-cDNA samples were mixed and heated for 3 min at 98°C before the samples were applied to the microarray slide containing 7738 70mer oligonucleotides printed in duplicate. Samples were hybridized for 18–20 h at 45°C and the slides were washed and dried before analysis. Data were collected using a GenePix 4000B scanner and analysed using GENEPIX PRO 6.0 (Axon Instruments, Foster City, CA). Data were further analysed in mAdb database at http://mAdb.niaid.nih.gov (NIAID). Three biological repeats were performed using three independent RNA sets isolated from cells cultured on different days and the dye-reverse hybridizations were performed for all three sets. One set of RNA was also subjected to technical repeats. All statistically significant genes were identified by SAM using a mean FDR of less than 4% (Tusher *et al*., 2001). Table 1 lists the statistically significant genes identified by SAM that have an average change of greater than 1.8-fold in *sre1*Δ strain upon $CoCl_2$ treatment. All statistically significant genes identified by SAM are given in Table S1 in *Supplementary material*.

Chromatin immunoprecipitation

Chromatin immunoprecipitation was performed as described previously using the ChIP assay kit (Upstate, Charlottesville, VA) with modifications (Todd *et al*., 2006). Briefly, 5×10^8 wild-type and *sre1*Δ cells were grown in the presence or absence of 0.6 mM $CoCl_2$ for 2 h. Cells were fixed in 1% formaldehyde, washed three times in sterile water and lyophilized overnight. Dried cells were lysed by vortexing with glass beads (425–600 mm, Sigma) at room temperature for 1–2 min and re-suspended in 1.5 ml of dilution buffer. Lysates were sonicated to shear DNA and pre-cleared by incubation with pre-blocked protein A/G beads (Upstate, Charlottesville, VA) for 30 min at 4°C. Beads were removed by centrifugation and 40 μl of pre-cleared lysate was reserved as 'input'. The lysates were incubated with 5 μl of anti-Sre1p polyclonal serum overnight at 4°C. Sre1p-DNA complexes were isolated by incubation with protein A/G beads (Upstate, Charlottesville, VA) for 2 h at 4°C, washed and DNA was recovered according to the manufacturer's instructions. Immunoprecipitated DNA was quantified by real-time PCR using Brilliant SYBR Green QPCR Master Mix (Stratagene, La Jolla, CA) and a MyiQ single-colour-detection thermal cycler (Bio-Rad, Hercules, CA). Three biological replicate experiments were performed and each replicate was analysed by quantitative PCR in triplicate. Primers used for the *ERG25* and *CCP1* promoters were designed ~100–300 bp upstream of start site (*ERG25*-ocb46-CGTGTGGGTTTTCCATTGCT, ocb47-CGATCCTCGGACTCTCAAA, *CCP1*-ocb67-CAATAGAGTCAGGGTCACATG, ocb68-CGGCGACATATCAACTTAGC).

Acknowledgements

This work was supported by funds from the intramural programme of the National Institute of Allergy and Infectious Diseases. This work was supported by a grant from the National Institutes of Health HL077588 (to P.J.E.). A.L.H. is a recipient of the American Heart Association Predoctoral Fellowship 0515394 U. P.J.E. is a recipient of a Burroughs Wellcome Fund Career Award in the Biomedical Sciences and a BWF Investigator in Pathogenesis of Infectious Disease.

References

Bard, M., Bruner, D.A., Pierson, C.A., Lees, N.D., Biermann, B., Frye, L., *et al.* (1996) Cloning and characterization of *ERG25*, the *Saccharomyces cerevisiae* gene encoding C-4 sterol methyl oxidase. *Proc Natl Acad Sci USA* **93:** 186–190.

Bennett, M.K., Lopez, J.M., Sanchez, H.B., and Osborne, T.F. (1995) Sterol regulation of fatty acid synthase promoter. Coordinate feedback regulation of two major lipid pathways. *J Biol Chem* **270:** 25578–25583.

Bruick, R.K., and McKnight, S.L. (2001) A conserved family of prolyl-4-hydroxylases that modify HIF. *Science* **294:** 1337–1340.

Burger, K., Gimpl, G., and Fahrenholz, F. (2000) Regulation of receptor function by cholesterol. *Cell Mol Life Sci* **57:** 1577–1592.

Burke, J.D., and Gould, K.L. (1994) Molecular cloning and characterization of the *Schizosaccharomyces pombe his3* gene for use as a selectable marker. *Mol Gen Genet* **242:** 169–176.

Chang, Y.C., and Kwon-Chung, K.J. (1994) Complementation of a capsule-deficient mutation of *Cryptococcus neoformans* restores its virulence. *Mol Cell Biol* **14:** 4912–4919.

Chang, Y.C., Wickes, B.L., and Kwon-Chung, K.J. (1995) Further analysis of the *CAP59* locus of *Cryptococcus neoformans*: structure defined by forced expression and description of a new ribosomal protein-encoding gene. *Gene* **167:** 179–183.

Chang, Y.C., Bien, C.M., Lee, H., Espenshade, P.J., and Kwon-Chung, K.J. (2007) *Cryptococcus neoformans* sterol regulatory element binding protein (Sre1p), a virulence factor that functions in oxygen sensing and sterol homeostasis. *Mol Microbiol* **64:** 614–629.

Chun, C.D., Liu, O.W., and Madhani, H.D. (2007) A link between virulence and homeostatic responses to hypoxia during infection by the human fungal pathogen *Cryptococcus neoformans*. *PLoS Pathog* **3:** e22.

Currie, B., Sanati, H., Ibrahim, A.S., Edwards, J.E., Jr, Casadevall, A., and Ghannoum, M.A. (1995) Sterol compositions and susceptibilities to amphotericin B of environmental *Cryptococcus neoformans* isolates are changed by murine passage. *Antimicrob Agents Chemother* **39:** 1934–1937.

Huang, Y., Du, K.M., Xue, Z.H., Yan, H., Li, D., Liu, W., *et al.* (2003) Cobalt chloride and low oxygen tension trigger differentiation of acute myeloid leukemic cells: possible mediation of hypoxia-inducible factor-1alpha. *Leukemia* **17:** 2065–2073.

Edman, J.C., and Kwon-Chung, K.J. (1990) Isolation of the *URA5* gene from *Cryptococcus neoformans* var. *neoformans* and its use as a selective marker for transformation. *Mol Cell Biol* **10:** 4538–4544.

Epstein, A.C., Gleadle, J.M., McNeill, L.A., Hewitson, K.S., O'Rourke, J., Mole, D.R., *et al.* (2001) *C. elegans* EGL-9 and mammalian homologs define a family of dioxygenases that regulate HIF by prolyl hydroxylation. *Cell* **107:** 43–54.

Forsburg, S.L. (1993) Comparison of *Schizosaccharomyces pombe* expression systems. *Nucleic Acids Res* **21:** 2955–2956.

Gachotte, D., Barbuch, R., Gaylor, J., Nickel, E., and Bard, M. (1998) Characterization of the *Saccharomyces cerevisiae ERG26* gene encoding the C-3 sterol dehydrogenase (C-4 decarboxylase) involved in sterol biosynthesis. *Proc Natl Acad Sci USA* **95:** 13794–13799.

Gachotte, D., Sen, S.E., Eckstein, J., Barbuch, R., Krieger, M., Ray, B.D., and Bard, M. (1999) Characterization of the *Saccharomyces cerevisiae* ERG27 gene encoding the 3-keto reductase involved in C-4 sterol demethylation. *Proc Natl Acad Sci USA* **96:** 12655–12660.

Ghannoum, M.A., Spellberg, B.J., Ibrahim, A.S., Ritchie, J.A., Currie, B., Spitzer, E.D., *et al.* (1994) Sterol composition of *Cryptococcus neoformans* in the presence and absence of fluconazole. *Antimicrob Agents Chemother* **38:** 2029–2033.

Goldberg, M.A., Glass, G.A., Cunningham, J.M., and Bunn, H.F. (1987) The regulated expression of erythropoietin by two human hepatoma cell lines. *Proc Natl Acad Sci USA* **84:** 7972–7976.

Goldberg, M.A., Dunning, S.P., and Bunn, H.F. (1988) Regulation of the erythropoietin gene: evidence that the oxygen sensor is a heme protein. *Science* **242:** 1412–1415.

Grasselli, F., Basini, G., Bussolati, S., and Bianco, F. (2005) Cobalt chloride, a hypoxia-mimicking agent, modulates redox status and functional parameters of cultured swine granulosa cells. *Reprod Fertil Dev* **17:** 715–720.

Hewitson, K.S., McNeill, L.A., Riordan, M.V., Tian, Y.M., Bullock, A.N., Welford, R.W., *et al.* (2002) Hypoxia-inducible factor (HIF) asparagine hydroxylase is identical to factor inhibiting HIF (FIH) and is related to the cupin structural family. *J Biol Chem* **277:** 26351–26355.

Horton, J.D., Shah, N.A., Warrington, J.A., Anderson, N.N., Park, S.W., Brown, M.S., and Goldstein, J.L. (2003) Combined analysis of oligonucleotide microarray data from transgenic and knockout mice identifies direct SREBP target genes. *Proc Natl Acad Sci USA* **100:** 12027–12032.

Hughes, A.L., Todd, B.L., and Espenshade, P.J. (2005) SREBP pathway responds to sterols and functions as an oxygen sensor in fission yeast. *Cell* **120:** 831–842.

Jaakkola, P., Mole, D.R., Tian, Y.M., Wilson, M.I., Gielbert, J., Gaskell, S.J., *et al.* (2001) Targeting of HIF-alpha to the von Hippel–Lindau ubiquitylation complex by O_2-regulated prolyl hydroxylation. *Science* **292:** 468–472.

Kennedy, M.A., Johnson, T.A., Lees, N.D., Barbuch, R., Eckstein, J.A., and Bard, M. (2000) Cloning and sequencing of the *Candida albicans* C-4 sterol methyl oxidase gene (*ERG25*) and expression of an ERG25 conditional lethal mutation in *Saccharomyces cerevisiae*. *Lipids* **35:** 257–262.

Kwon-Chung, K.J., and Bennett, J.E. (1992) *Medical Mycology*. Philadelphia, PA: Lea & Febiger.

Kwon-Chung, K.J., Edman, J.C., and Wickes, B.L. (1992) Genetic association of mating types and virulence in *Cryptococcus neoformans*. *Infect Immun* **60:** 602–605.

Lee, H., Chang, Y.C., and Kwon-Chung, K.J. (2005) *TUP1* disruption reveals biological differences between *MATa* and *MATalpha* strains of *Cryptococcus neoformans*. *Mol Microbiol* **55:** 1222–1232.

Lees, N.D., Skaggs, B., Kirsch, D.R., and Bard, M. (1995) Cloning of the late genes in the ergosterol biosynthetic pathway of *Saccharomyces cerevisiae* – a review. *Lipids* **30:** 221–226.

Lees, N.D., Bard, M., and Kirsch, D.R. (1999) Biochemistry and molecular biology of sterol synthesis in *Saccharomyces cerevisiae*. *Crit Rev Biochem Mol Biol* **34:** 33–47.

Li, L., and Kaplan, J. (1996) Characterization of yeast methyl sterol oxidase (ERG25) and identification of a human homologue. *J Biol Chem* **271:** 16927–16933.

Mondon, P., Chang, Y.C., Varma, A., and Kwon-Chung, K.J. (2000) A novel episomal shuttle vector for transformation of *Cryptococcus neoformans* with the *ccdB* gene as a positive selection marker in bacteria. *FEMS Microbiol Lett* **187:** 41–45.

Moreno, S., Klar, A., and Nurse, P. (1991) Molecular genetic analysis of fission yeast *Schizosaccharomyces pombe*. *Methods Enzymol* **194:** 795–823.

Odds, F.C., De Backer, T., Dams, G., Vranckx, L., and Woestenborghs, F. (1995) Oxygen as limiting nutrient for growth

of *Cryptococcus neoformans*. *J Clin Microbiol* **33:** 995–997.

Rawson, R.B., DeBose-Boyd, R., Goldstein, J.L., and Brown, M.S. (1999) Failure to cleave sterol regulatory element-binding proteins (SREBPs) causes cholesterol auxotrophy in Chinese hamster ovary cells with genetic absence of SREBP cleavage-activating protein. *J Biol Chem* **274:** 28549–28556.

Salnikow, K., Donald, S.P., Bruick, R.K., Zhitkovich, A., Phang, J.M., and Kasprzak, K.S. (2004) Depletion of intracellular ascorbate by the carcinogenic metals nickel and cobalt results in the induction of hypoxic stress. *J Biol Chem* **279:** 40337–40344.

Semenza, G.L. (2004) Hydroxylation of HIF-1: oxygen sensing at the molecular level. *Physiology (Bethesda)* **19:** 176–182.

Shibayama, N., Morimoto, H., and Miyazaki, G. (1986) Oxygen equilibrium study and light absorption spectra of Ni(II)–Fe(II) hybrid hemoglobins. *J Mol Biol* **192:** 323–329.

Sinclair, P., Gibbs, A.H., Sinclair, J.F., and de Matteis, F. (1979) Formation of cobalt protoporphyrin in the liver of rats. A mechanism for the inhibition of liver haem biosynthesis by inorganic cobalt. *Biochem J* **178:** 529–538.

Sinclair, P.R., Sinclair, J.F., Bonkowsky, H.L., Gibbs, A.H., and De Matteis, F. (1982) Formation of cobalt protoporphyrin by chicken hepatocytes in culture. Relationship to decrease of 5-aminolaevulinate synthase caused by cobalt. *Biochem Pharmacol* **31:** 993–999.

Theis, T., and Stahl, U. (2004) Antifungal proteins: targets, mechanisms and prospective applications. *Cell Mol Life Sci* **61:** 437–455.

Todd, B.L., Stewart, E.V., Burg, J.S., Hughes, A.L., and Espenshade, P.J. (2006) Sterol regulatory element binding protein is a principal regulator of anaerobic gene expression in fission yeast. *Mol Cell Biol* **26:** 2817–2831.

Triantafyllou, A., Liakos, P., Tsakalof, A., Georgatsou, E., Simos, G., and Bonanou, S. (2006) Cobalt induces hypoxia-inducible factor-1alpha (HIF-1alpha) in HeLa cells by an iron-independent, but ROS-, PI-3K- and MAPK-dependent mechanism. *Free Radical Research* **40:** 847–856.

Tusher, V.G., Tibshirani, R., and Chu, G. (2001) Significance analysis of microarrays applied to the ionizing radiation response. *Proc Natl Acad Sci USA* **98:** 5116–5121.

Vengellur, A., Woods, B.G., Ryan, H.E., Johnson, R.S., and LaPres, J.J. (2003) Gene expression profiling of the hypoxia signaling pathway in hypoxia-inducible factor 1alpha null mouse embryonic fibroblasts. *Gene Expr* **11:** 181–197.

Wang, G., Hazra, T.K., Mitra, S., Lee, H.M., and Englander, E.W. (2000) Mitochondrial DNA damage and a hypoxic response are induced by $CoCl_2$ in rat neuronal PC12 cells. *Nucleic Acids Res* **28:** 2135–2140.

Wang, G.L., and Semenza, G.L. (1993) Characterization of hypoxia-inducible factor 1 and regulation of DNA binding activity by hypoxia. *J Biol Chem* **268:** 21513–21518.

Supplementary material

The following supplementary material is available for this article:

Table S1. All statistically significant genes obtained from SAM analysis whose expression was changed in the *sre1* deletant when treated with 0.6 mM $CoCl_2$ for 2 h. NA represents features that were flagged absent or bad by GenePix or manually.

This material is available as part of the online article from:
http://www.blackwell-synergy.com/doi/abs/10.1111/j.1365-2958.2007.05844.x
(This link will take you to the article abstract).

Please note: Blackwell Publishing is not responsible for the content or functionality of any supplementary materials supplied by the authors. Any queries (other than missing material) should be directed to the corresponding author for the article.